

## Electronic structures of iron and cobalt pyrites

G. L. Zhao, J. Callaway, and M. Hayashibara\*

*Department of Physics and Astronomy, Louisiana State University, Baton Rouge, Louisiana 70803-4001*

(Received 3 May 1993)

We report self-consistent, all-electron, local-spin-density calculations of energy bands of iron and cobalt pyrites ( $\text{FeS}_2$  and  $\text{CoS}_2$ ). We find  $\text{FeS}_2$  to be a moderately small-band-gap semiconductor and  $\text{CoS}_2$  to be an almost half-metallic ferromagnet. The predicted Fermi surface of  $\text{CoS}_2$  is described.

### I. INTRODUCTION

The late transition-metal pyrites (formula  $MS_2$  where  $M = \text{Fe, Co, Ni, Cu, and Zn}$ ) form a series of compounds with extremely interesting electrical and magnetic properties. A small selection of relevant papers are listed below.<sup>1-6</sup> Iron pyrite (fool's gold) is a semiconductor with a relatively small band gap. The iron is not magnetic. Cobalt pyrite is an itinerant electron ferromagnet; nickel pyrite is an antiferromagnetic semiconductor; copper pyrite is metallic with a low-temperature transition to a superconducting state, while zinc pyrite is a wide-band-gap, nonmagnetic insulator. The compounds have been discussed in terms of the filling of an upper  $e_g$  band<sup>7</sup> as one goes from  $\text{FeS}_2$  (where it is empty) to  $\text{ZnS}_2$  (where it is completely full), and a simple picture based on a one-band Hubbard model<sup>8</sup> has been invoked.<sup>3</sup> The crystal structure, common to all these materials, is cubic.

The properties of these materials contrast strongly with what has been found for high-temperature superconductors (which, in contrast, involve oxygen and copper, and have important two-dimensional features). In the pyrites, doping holes into an antiferromagnetic insulator leads to ferromagnetism rather than superconductivity, while the electron-doped system is a low-temperature superconductor.

The electronic structure of the pyrites has not been intensively investigated, there being only a relatively small number of band calculations,<sup>9-12</sup> mainly emphasizing  $\text{FeS}_2$ . The calculations in Refs. 10-12 agree qualitatively in many respects in regard to the bands of  $\text{FeS}_2$ , although there are important quantitative variations in regard to bandwidths and separations.

In this paper we report the results of the application of a self-consistent tight-binding method to  $\text{FeS}_2$  and  $\text{CoS}_2$ , based on the local-spin-density approximation.

The results of our calculation for  $\text{FeS}_2$ , which are described in Sec. III, support the same general picture of the band structure that has been presented previously in Refs. 10-12. There are significant differences in details in regard to the region of the energy gap between the upper valence and lowest conduction band, and specifically in regard to the location of the band maxima and minima. These differences should be resolvable by suitable experiments. Our calculation for  $\text{CoS}_2$  is the first to describe a predicted Fermi surface. We find that  $\text{CoS}_2$  just misses being a half-metallic ferromagnet in the sense that the number of occupied minority-spin states in the

upper band is quite small compared to the number of majority-spin states.

The remainder of this paper is organized as follows. Our calculational procedures are briefly described in Sec. II. Section III contains our results for  $\text{FeS}_2$ ; Sec. IV, those for  $\text{CoS}_2$ . A brief summary is presented in Sec. V.

### II. CALCULATIONAL PROCEDURES

The crystal structure of pyrite materials is illustrated in Fig. 1(a). The four metal atoms are located at posi-

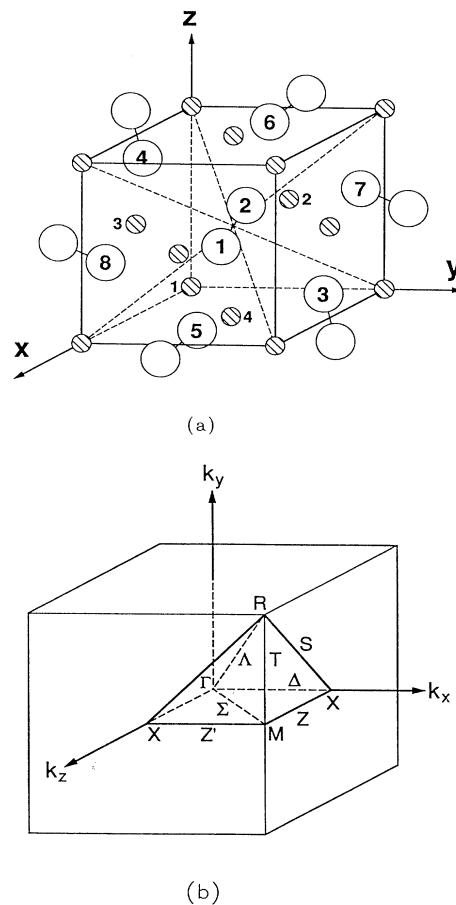


FIG. 1. (a) Crystal structure of pyrite compounds, (b) Brillouin zone showing irreducible wedge with points and lines of symmetry.

tions (0,0,0), (0,1/2,1/2), (1/2,0,1/2), and (1/2,1/2,0). The eight sulfur atoms are in position  $\pm(u, u, u)$ ,  $\pm(u + 1/2, 1/2 - u, \bar{u})$ ,  $\pm(\bar{u}, u + 1/2, 1/2 - u)$ , and  $\pm(1/2 - u, \bar{u}, u + 1/2)$ . We use values of the lattice parameter and of  $u$  taken from Wyckoff.<sup>13</sup> These are listed in Table I.

The space group is  $T_h^6(Pa3)$ . There are only 24 operations in the point group  $T_h$ , so that the irreducible wedge of the Brillouin zone is twice as big as in the more familiar monoatomic case. The zone and wedge are illustrated in Fig. 1(b). One significant difference, in comparison with the simple cubic case is that the lines connecting  $X$  with  $M$  are of two types;  $Z(1, x, 0)$  and  $Z'(1, 0, x)$ . Energies along  $Z$  and  $Z'$  are not identical.

Our calculation employs the self-consistent linear combination of atomic orbitals (LCAO) procedure described by Feibelman, Appelbaum, and Hamann.<sup>14</sup> This procedure has been used by several groups, and has been found to be of comparable accuracy to other first-principles methods.<sup>14-18</sup> For example, the calculated electronic structures of  $\beta$ -phase NiAl and NiTi using the first-principles LCAO method agree with other carefully performed computations.<sup>19,20</sup> In work not yet published, we have found excellent agreement in regard to the band structure of  $YBa_2Cu_3O_7$  between the results of this LCAO code and that obtained by other methods.<sup>21</sup> We believe that this method is appropriate in view of the structure and composition of the pyrites.

In the first step, one constructs atomic wave functions using a Gaussian orbital basis in the self-consistent local-density calculation. The radial wave functions for a state of angular momentum  $l$  is written as

$$R_{nl}(r) = r^l \sum_{i=1}^N C_{ni} e^{-\alpha_i r^2},$$

where  $N=19$  for  $s$  and  $p$  states and 16 for  $d$  states. An even tempered set of exponents is employed with the minimum  $\alpha_i$  being 0.05 and the maximum  $1.4 \times 10^6$ . Since the valence wave functions of an isolated atom have long tails, the inclusion of small values of  $\alpha$  is necessary to represent the atomic charge density accurately.

However, in a solid, the inclusion of long tails of atomic wave functions is likely to lead to overcompleteness problems rather than to increased accuracy. Therefore, after an accurate self-consistent atomic potential has been obtained, we determined the orbital basis set for the solid-state calculations by solving the isolated atom Schrödinger equations variationally with this potential but eliminating the two smallest  $\alpha_i$ 's in the Gaussian basis.

The  $1s$ ,  $2s$ ,  $2p$ ,  $3s$ , and  $3p$  atomic orbitals of iron and cobalt and the  $1s$ ,  $2s$ , and  $2p$  orbitals of sulfur were considered to be core states. A rigid-core approximation was made concerning these orbitals in the self-consistent cal-

ulation. These states are quite localized and do not broaden significantly in the solid. The metal  $3d$ ,  $4s$ , and  $4p$  orbitals and the sulfur  $3s$ ,  $3p$ , and  $4s$  orbitals were included in the self-consistent calculation for both cases. As we were concerned about some differences between our results and those of previous authors for  $FeS_2$ , we repeated the self-consistent calculation for this material including additionally a  $4p$  and a  $5s$  orbital on iron and a  $4p$  on sulfur. The smaller basis has dimension 76; the larger, 104. We did not find appreciable changes.

The self-consistent calculations employed a grid of  $76k$  points in the irreducible Brillouin zone. A comparison with results based on  $24k$  points showed a difference in total energy of only 0.0023 Ry per cell. We believe this indicates satisfactory convergence with respect to the number of  $k$  points in the zone.

The exchange-correlation potential used in this work was that due to von Barth and Hedin as modified by Moruzzi, Janak, and Williams.<sup>22</sup>

### III. RESULTS: $FeS_2$

In general, the electronic structures of  $FeS_2$  and  $CoS_2$  are quite similar, apart from the differences resulting from the presence of an extra electron and the exchange splitting resulting from ferromagnetism in  $CoS_2$ .

Figures 2(a) and 2(b) present the band structure and density of states of  $FeS_2$  on a coarse energy scale to give an overall view of the electronic structure. Figures 3(a) and 3(b) show the region around the Fermi energy on a finer scale which makes details of the highest valence band and lowest conduction band more apparent.  $FeS_2$  is predicted to be a relatively narrow band-gap semiconductor. The valence-band maximum is at the  $X$  point (100), and the conduction-band minimum is at  $\Gamma$ . The indirect band gap between these two points is calculated to be 0.59 eV. We find the smallest direct gap to be 0.74 eV, at the zone center. Our results differ from those of Folkerts *et al.*, who found the highest occupied state not to be on a high symmetry line, and the lowest unoccupied state to be at about 0.7 of the distance from the center to the zone face along (1,1,1).

Unfortunately, there is no consensus in regard to the experimental band gap. The situation was summarized in a note by Ferrer *et al.*<sup>23</sup> who observe that many different values have been reported, most of which are in the range of 0.9–1.2 eV. Neither is there agreement among experimentalists as to whether the (lowest) gap is direct or indirect, although many authors propose that the gap is indirect.<sup>23</sup> A glance at Fig. 3(b) shows that the conduction-band density of states rises rapidly at about 1.2 eV above the valence-band maximum, but there is a long tail which extends down to 0.59 eV. Since the valence bands are rather flat, the optical absorption would be expected to increase rapidly at about 1.2 eV. The large energy difference between this and the smaller indirect gap may contribute to the difficulties experienced in interpreting the observed optical absorption.

Figure 4 shows the contributions of different elements of the orbital basis to the density of states. This figure should be considered in conjunction with Figs. 2(a) and

TABLE I. Crystal structure parameters.

	$a$	$u$
$FeS_2$	5.407 Å	0.386
$CoS_2$	5.524 Å	0.389

2(b). Starting at about 20 eV below the highest occupied state, we see a pair of bands, principally involving sulfur  $s$  orbitals. According to Bullett,<sup>10</sup> these bands are associated with bonding and antibonding pairs of orbitals on the  $S_2$  pairs. These bands are split by about 3 eV and are separated by 4 eV from a complex structure of sulfur  $3p$  bands with a small admixture of iron  $3d$  functions. These bands cover a range of about 5.5 eV, and are separated by about 3 eV from a narrow (1.4 eV wide) band based principally on Fe  $t_{2g}$  hybridized with some sulfur  $p$  orbitals. These band positions and separations seem to be in reasonable accord with the x-ray photoemission spectroscopy measurements of van der Heide *et al.*<sup>24</sup> and of Folkerts *et al.*<sup>12</sup>

The lowest conduction band is not so narrow (about 3 eV wide), and is formed from a combination of Fe  $e_g$  and  $t_{2g}$  orbitals hybridized with sulfur  $p$ . The lowest minimum (at  $\Gamma$ ) is well separated from the rest of these bands, and the band structure around  $\Gamma$  is reasonably parabolic (the effective mass at  $\Gamma$  is about  $0.35 m_0$ ). An unusual feature is the 6 eV gap which separates this band from the higher conduction bands involving metal  $s$  and  $p$  orbitals. A gap of about 4 eV seems to be present in the bremsstrahlung isochromat spectroscopy measurements of Folkerts *et al.*<sup>12</sup>

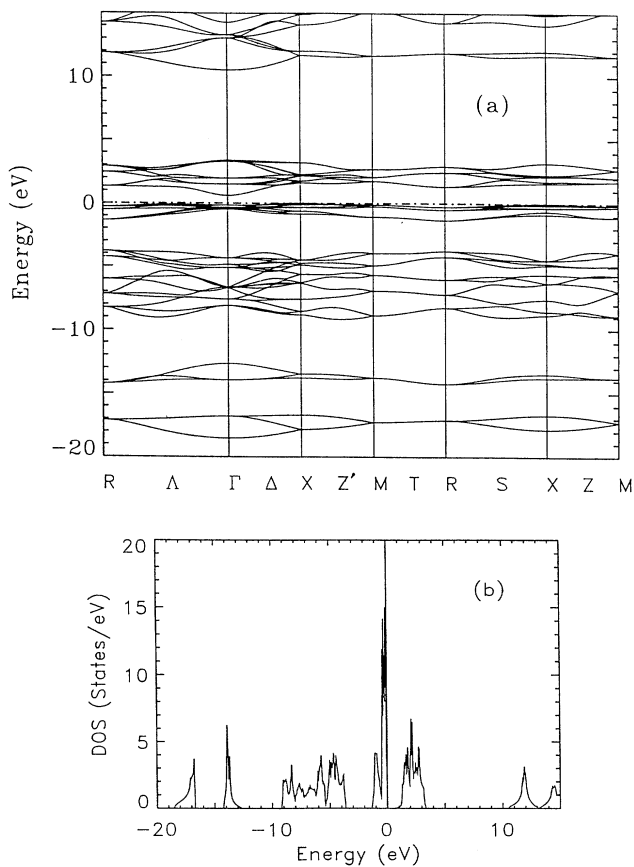


FIG. 2. (a) Energy bands of  $FeS_2$  on a coarse energy scale, (b) density of states. The zero of energy has been set at the highest occupied state.

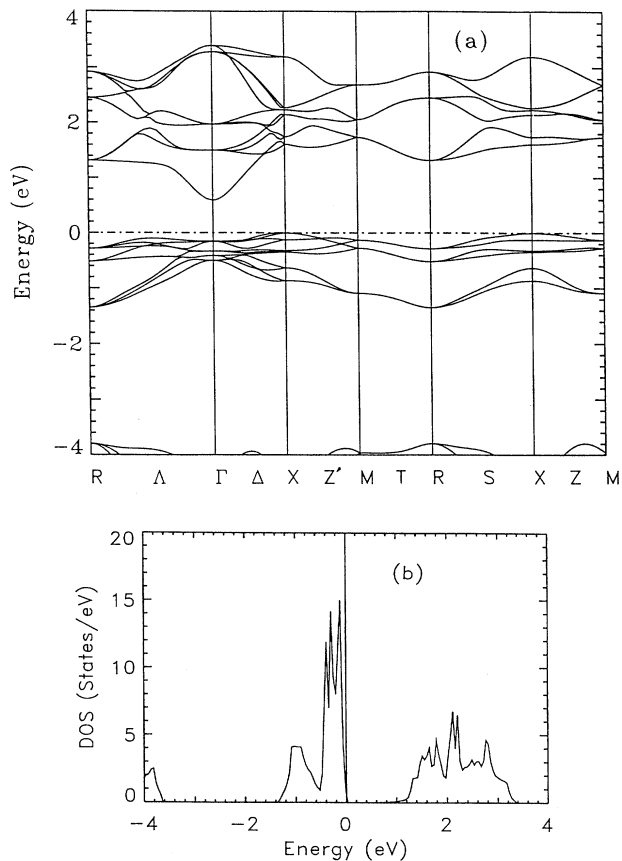


FIG. 3. (a) Energy bands of  $FeS_2$  on a finer energy scale, (b) density of states.

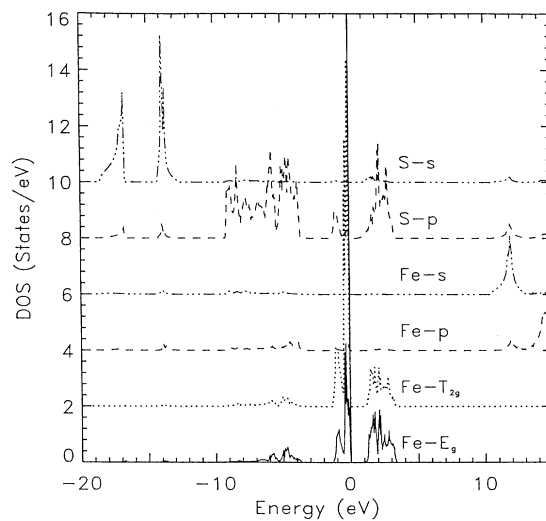


FIG. 4. Basis set decomposition of the density of states of  $FeS_2$ . Orbital contributions have been offset for clarity of presentation.

IV. RESULTS: CoS<sub>2</sub>

Our self-consistent, spin-polarized calculation yields a ferromagnetic ground state for CoS<sub>2</sub>. We find a magnetic moment of 0.92μ<sub>B</sub> per Co atom at T=0, which is close to the experimental value (0.9μ<sub>B</sub>).<sup>2</sup>

The density of states is shown for a wide energy range in Fig. 5(a), and on an expanded scale, emphasizing the region close to the Fermi energy in Fig. 5(b). The bands corresponding to the lowest 3 peaks in Fig. 5(a), which are formed primarily from sulfur s and p orbitals, resemble those in FeS<sub>2</sub> except for a shift to lower energy of roughly 1 eV. Their spin splitting is small. We emphasize here the bands in the region of the Fermi energy, which are illustrated in Fig. 6. The orbital basis decomposition of the density of states is similar for all bands to that shown in Fig. 4 for FeS<sub>2</sub>.

The lowest pair of spin-split bands in Fig. 6 is based principally on Co 3d orbitals. The exchange splitting of these bands varies between about 0.6 eV for the lower states and 0.8 eV for the higher. The Fermi energy is in the upper band pair which contains both Co e<sub>g</sub> and t<sub>2g</sub> orbitals hybridized with sulfur 3p. The exchange splitting is in the range of 0.6–0.8 eV at the bottom of this complex, but is smaller at the top (0.0–0.2 eV), where sulfur p orbitals contribute strongly to the wave functions.

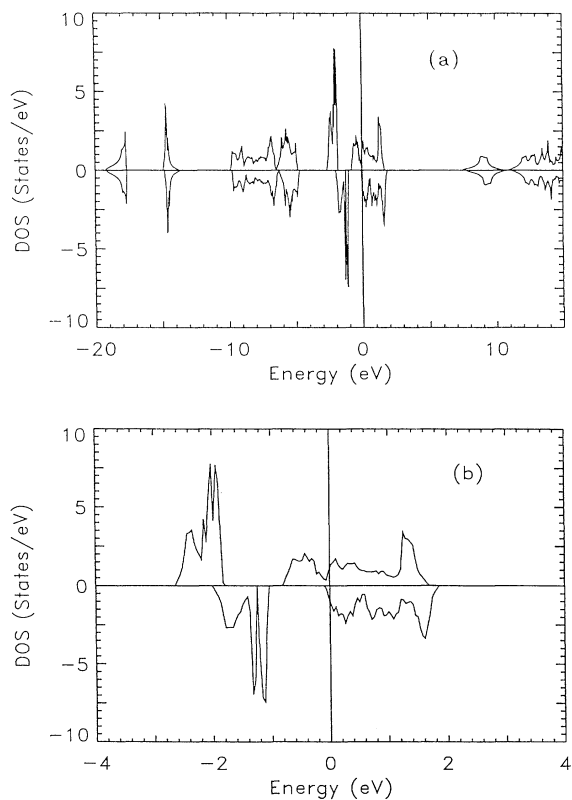


FIG. 5. (a) Density of states for CoS<sub>2</sub> on a coarse energy scale. The top portion corresponds to majority-spin, the lower to minority-spin states. The zero of energy is taken at the Fermi energy, (b) density of states on a finer energy scale.

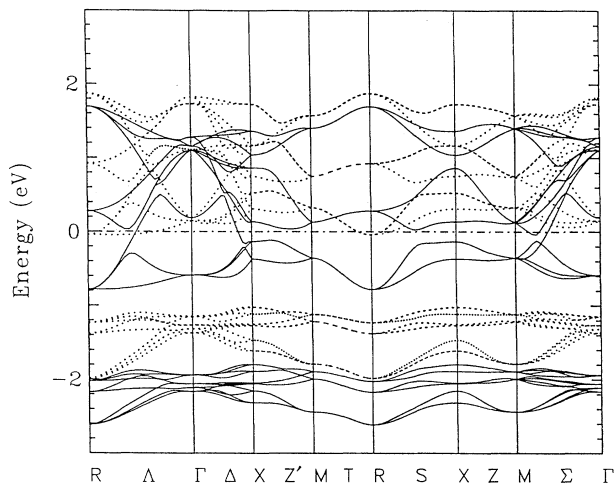


FIG. 6. Energy bands of CoS<sub>2</sub>: Solid lines, majority-spin states (“up”), dashed lines minority spins (“down”). The Fermi energy has been used as the zero of the energy scale.

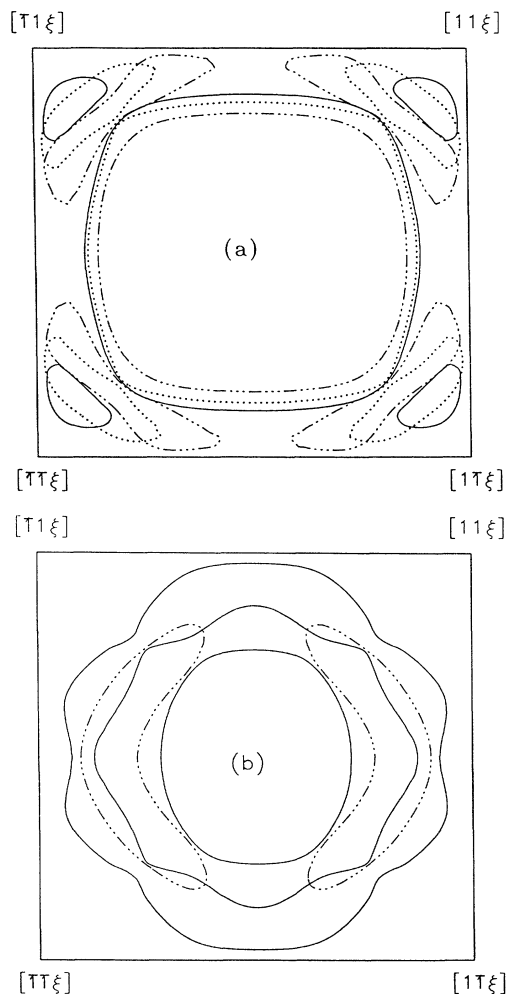


FIG. 7. Cross sections of the majority-spin Fermi surface in k<sub>x</sub>-k<sub>y</sub> planes: (a) solid line, ξ=k<sub>z</sub>=0; dots, k<sub>z</sub>=0.3π/a; dashed-dot line, k<sub>z</sub>=0.5π/a, (b) solid line, ξ=k<sub>z</sub>=0.7π/a; dashed-dot line, k<sub>z</sub>=0.9π/a.

It will be observed from both Figs. 5(b) and 6 that only a small number of minority spin states are occupied. CoS<sub>2</sub> just misses being a half-metallic ferromagnet (in which case there would be no occupied minority-spin states in this band). We will describe CoS<sub>2</sub> as almost a half-metallic ferromagnet. It is plausible to suppose that the half-metallic condition might be attained for somewhat smaller occupancy of states in this band, as would be expected in the mixed system Fe<sub>x</sub>Co<sub>1-x</sub>S<sub>2</sub>. Experimental results indicate that this probably occurs for  $x \geq 0.05$ .<sup>2</sup>

Although there do not yet appear to be any measurements of the Fermi surface of CoS<sub>2</sub>, we think it will be useful to present some calculated results for this with the hope that experimental investigation will be encouraged.

Cross sections of the majority-spin Fermi surface in  $k_x$ - $k_y$  planes are shown for three different values of  $k_z$  in Fig. 7(a). Two majority- (up) spin bands cross the Fermi energy. Each forms its own portion of Fermi surface. The large central portion is a rounded square. For  $k_z=0$ , there are small, electron pockets near the corners of the zone face which, however, do not touch the boundary. As  $k_z$  increases, the central portion shrinks and the electron pockets expand. When  $k_z$  increases to  $0.7\pi/a$  the pockets join to form a cage around a shrunken central portion, Fig. 7(b). Further increase of  $k_z$  leads to disappearance of the central figure and the separation of the cage into elongated pockets. The spin-up surface does not reach  $k_z=\pi/a$ .

A minority- (down) spin band intersects the Fermi energy near  $R$ . The resulting Fermi surface (Fig. 8) consists of four tubes which are connected at  $R$  to form a cross shaped figure, and extend into the zone to  $k_z=0.4\pi/a$ , where the structure terminates.

## V. SUMMARY

We have performed self-consistent local-spin-density electronic structure calculations using a LCAO method for iron and cobalt pyrites (FeS<sub>2</sub> and CoS<sub>2</sub>). We find, in

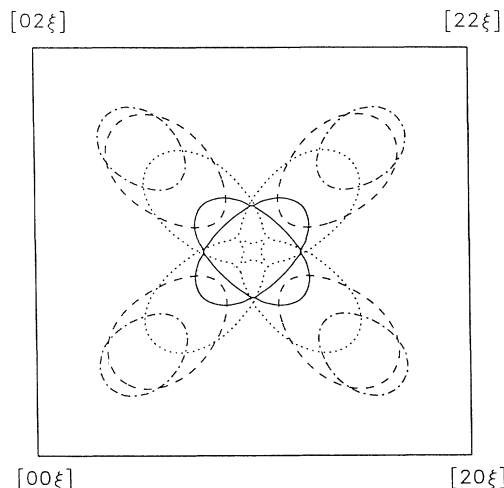


FIG. 8. Minority-spin Fermi surface in  $k_x$ - $k_y$  planes but centered at  $[1,1,\xi]$ . Solid line;  $\xi=k_z=\pi/a$ ; dots,  $k_z=0.8\pi/a$ ; dashes,  $k_z=0.6\pi/a$ ; dash-dot line,  $k_z=0.4\pi/a$ .

agreement with experiment, that FeS<sub>2</sub> is a moderately small-band-gap semiconductor and that CoS<sub>2</sub> is an itinerant electron ferromagnet, almost half metallic. Although our calculated gap for FeS<sub>2</sub> is probably significantly smaller than the actual value (which is apparently not accurately known at this time) we believe that our predictions that the gap is indirect and that the highest valence-band maximum and lowest conduction-band minimum are located at  $X$  and  $\Gamma$  may be reliable. The calculated magnetic moment of CoS<sub>2</sub> agrees adequately with experiment. We have described the rather complicated Fermi surface of this material, which has not yet been investigated experimentally.

## ACKNOWLEDGMENT

This research was supported in part by the National Science Foundation under Grant No. DMR91-20166.

\*Permanent address: Energy Research Laboratory, Hitachi Ltd., Hitachi-shi, Ibaraki-ken 316, Japan.

<sup>1</sup>T. A. Bither, R. J. Bouchard, W. H. Cloud, P. C. Donohue, and W. J. Siemons, *Inorg. Chem.* **7**, 2208 (1968).

<sup>2</sup>H. S. Jarrett, W. H. Cloud, R. J. Bouchard, S. R. Butler, C. G. Frederick, and J. L. Gillson, *Phys. Rev. Lett.* **21**, 617 (1968).

<sup>3</sup>S. Ogawa, S. Waki, and T. Teranishi, *Int. J. Magn.* **5**, 349 (1974).

<sup>4</sup>K. Kikuchi, T. Miyadi, H. Itoh, and T. Fukui, *J. Phys. Soc. Jpn.* **45**, 444 (1978).

<sup>5</sup>J. A. Wilson and G. D. Pitt, *Philos. Mag.* **23**, 1297 (1971).

<sup>6</sup>R. A. Munson, W. DeSorbo, and J. S. Kouvel, *J. Chem. Phys.* **47**, 1769 (1967).

<sup>7</sup>J. B. Goodenough, *J. Solid State Chem.* **5**, 144 (1972).

<sup>8</sup>D. R. Penn, *Phys. Rev.* **142**, 350 (1966).

<sup>9</sup>M. A. Khan, *J. Phys. C* **9**, 81 (1976).

<sup>10</sup>D. W. Bullett, *J. Phys. C* **15**, 6163 (1982).

<sup>11</sup>S. Lauer, A. E. Trautwein, and F. E. Harris, *Phys. Rev. B* **29**, 6774 (1984).

<sup>12</sup>W. Folkerts, G. A. Sawatzky, C. Haas, R. A. de Groot, and F. U. Hillebrecht, *J. Phys. C* **20**, 4135 (1987).

<sup>13</sup>R. W. G. Wyckoff, *Crystal Structures* (Interscience, New York, 1965), Vol. 1.

<sup>14</sup>P. J. Feibelman, J. A. Appelbaum, and D. R. Hamann, *Phys. Rev. B* **20**, 1433 (1979).

<sup>15</sup>B. N. Harmon, W. Weber, and D. R. Hamann, *Phys. Rev. B* **25**, 1109 (1982).

<sup>16</sup>W. Y. Ching, Yongnian Xu, Guang-Lin Zhao, K. W. Wong, and F. Zandiehndem, *Phys. Rev. Lett.* **59**, 1333 (1987).

<sup>17</sup>G. L. Zhao, T. C. Leung, B. N. Harmon, M. Keil, M. Muller, and W. Weber, *Phys. Rev. B* **40**, 7999 (1989).

<sup>18</sup>G. L. Zhao and B. N. Harmon, *Phys. Rev. B* **45**, 2818 (1992).

<sup>19</sup>S. C. Lui, J. W. Davenport, E. W. Plummer, D. M. Zehner, and D. W. Fernando, *Phys. Rev. B* **42**, 1582 (1990).

- <sup>20</sup>K. J. Kim, B. N. Harmon, and D. W. Lynch, *Phys. Rev. B* **43**, 1948 (1991).
- <sup>21</sup>W. E. Pickett, R. E. Cohen, and H. Krakauer, *Phys. Rev. B* **42**, 8764 (1990).
- <sup>22</sup>U. von Barth and L. Hedin, *J. Phys. C* **5**, 1629 (1972); V. L. Moruzzi, J. F. Janak, and A. R. Williams, *Calculated Elec-*

*tronic Properties of Metals* (Pergamon, New York, 1978).

- <sup>23</sup>I. J. Ferrer, D. M. Nevskaia, C. de las Heras, and C. Sanchez, *Solid State Commun.* **74**, 913 (1990).
- <sup>24</sup>H. van der Heide, R. Hemmel, C. F. van Bruggen, and C. Haas, *J. Solid State Chem.* **33**, 17 (1980).